Empirical Constraints on the Nucleosynthesis of Nitrogen

James W. Johnson,[1★] David H. Weinberg,[1,2,3] Fiorenzo Vincenzo,[1,2] Jonathan C. Bird,[4] and and Emily J. Griffith[1]

[1] Department of Astronomy, The Ohio State University, 140 W. 18th Ave., Columbus, OH, 43210, USA
[2] Center for Cosmology and Astroparticle Physics (CCAPP), The Ohio State University, 191 W. Woodruff Ave., Columbus, OH, 43210, USA
[3] Institute for Advanced Study, 1 Einstein Dr., Princeton, NJ, 08540, USA
[4] Department of Physics & Astronomy, Vanderbilt University, 2301 Vanderbilt Place, Nashville, TN, 37235, USA

Accepted XXX; Received YYY; in original form ZZZ

ABSTRACT

We use a multi-ring galactic chemical evolution model to probe the astrophysical production of nitrogen (N) in the Milky Way. This approach treats individual annuli in the Galaxy disc as conventional one-zone models, and to include the effects of radial migration, stellar populations move between annuli in a manner based on star particles from a hydrodynamical simulation. We find that some recent AGB star yield tables are able to reproduce the gas-phase [N/O]-[O/H] relation as observed only if a substantial fraction of massive stars collapse to black holes. If instead most massive stars explode as supernovae, we must artificially increase N yields from AGB stars by factors of 2 – 3 to offset the additional oxygen. We demonstrate that, with a viable set of AGB star yields, our model is able to reproduce many of the observed correlations between N, O, and Fe abundances for stars when the N abundances are corrected for internal mixing processes within stars. With any of these yields, N production timescales are sufficiently short such that stellar migration is only a minimal source of intrinsic scatter in the observed [N/O]-[O/H] relation. Modest variations in the star formation rate and star formation efficiency produce considerably larger variations in the gas phase N and O abundances, consistent with previous observational arguments. Our models run using the publicly available `Versatile Integrator for Chemical Evolution` (`VICE`; `https://pypi.org/project/vice`).

Key words: methods: numerical – galaxies: abundances, evolution, star formation, stellar content

1 INTRODUCTION

From a nucleosynthesis perspective, nitrogen (N) is a unique element. Along with carbon (C) and helium (He), it is one of only three elements produced in asymptotic giant branch (AGB) stars that are lighter than iron peak nuclei (Johnson 2019). N is also a by-product of the nuclear fusion reactions converting hydrogen (H) into He in stars more massive than the sun with nonzero metallicity. The CNO cycle[1] catalyses the proton-proton chain of nuclear reactions (e.g. Suliga, Shalgar & Fuller 2020) using C, N, and oxygen (O) target nuclei. The slowest component of this chain reaction by far is the ^{14}N(p,γ)^{15}O component. As a consequence of this bottleneck, to first order the effect of the CNO cycle is to convert all of the C and O isotopes present in a star's core into ^{14}N. Furthermore, N is among a select group of elements whose observed abundances in stellar spectra often do not reflect the star's birth abundances. Because N is produced in main sequence stars via the CNO cycle, its abundances in a star's core become enhanced relative to what the star was born with. Upon becoming a red giant, internal mixing processes (i.e. dredge-up) bring this N-enhanced material to the photosphere. This phenomenon is both expected from theoretical models and observed in open and globular clusters (Gilroy 1989; Korn et al. 2007; Lind et al. 2008; Souto et al. 2018, 2019; Vincenzo et al. 2021).

Both observationally and theoretically, N is among the more well-studied elements. Of particular interest in this paper is the correlation between the abundances of N and O, usually observed in the gas phase. In Fig. 1, we present a compilation of such measurements:

1. HII regions in the first six CHAOS[2] galaxies (NGC 3184, NGC 628, NGC 5194, NGC 5457, M101, NGC 2403; Berg et al. 2020; Skillman et al. 2020; Rogers et al. 2021).
2. HII regions in nearby NGC spirals (Pilyugin, Vílchez & Thuan 2010).
3. HII regions in blue, diffuse star forming dwarf galaxies (Berg et al. 2012; Izotov, Thuan & Guseva 2012; James et al. 2015).
4. Local stars and HII regions (Dopita et al. 2016).
5. Galactic and extragalactic HII regions (Henry, Edmunds & Köppen 2000).
6. Star-forming regions in 550 nearby galaxies in the MaNGA IFU[3] survey (Belfiore et al. 2017).

Despite intrinsic scatter and some systematic variation in how the

★ Contact e-mail: johnson.7419@osu.edu
[1] ^{12}C(p, γ)^{13}N(β^+, ν_e)^{13}C(p, γ) ^{14}N(p, γ)^{15}O(β^+, ν_e)^{15}N(p, α) ^{12}C

[2] CHAOS: CHemical Abundances of Spirals (Berg et al. 2015)
[3] MaNGA: Mapping Nearby Galaxies at Apache Point Observatory (Bundy et al. 2015). IFU: Integral Field Unit.

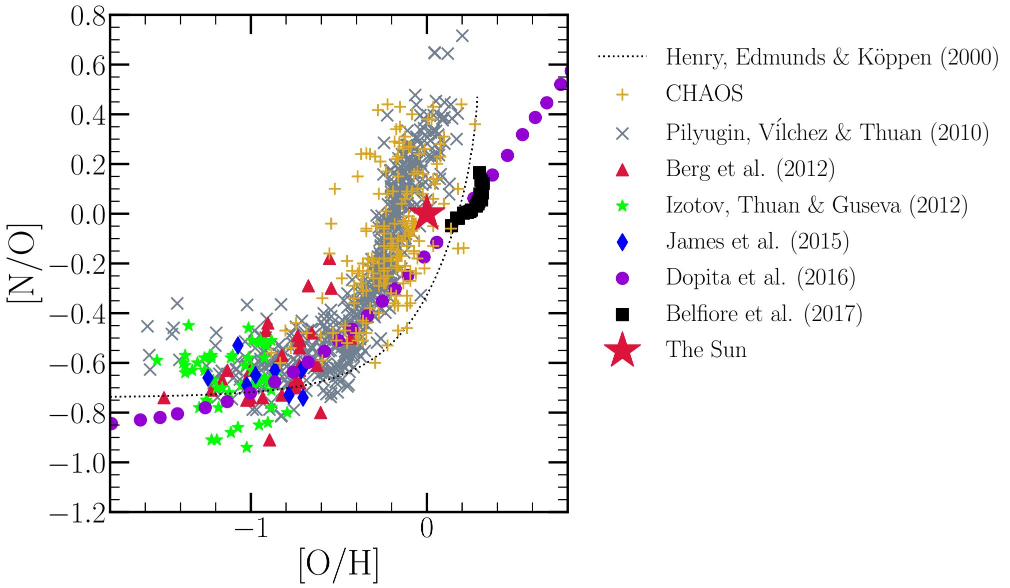

Figure 1. The [N/O]-[O/H] relation as observed in different galactic environments: HII regions from the first six CHAOS galaxies (golden +'s: NGC 3184, NGC 628, NGC 5194, NGC 5457, M101, and NGC 2403; Berg et al. 2020; Skillman et al. 2020; Rogers et al. 2021) and other nearby NGC spiral galaxies (grey X's; Pilyugin et al. 2010), HII regions in blue diffuse star forming dwarf galaxies (red triangles: Berg et al. 2012; green stars: Izotov et al. 2012; blue diamonds: James et al. 2015), in local stars and HII regions (purple circles: Dopita et al. 2016), and in the MaNGA IFU survey (black squares: Belfiore et al. 2017). The fit to [N/O] as a function of [O/H] in Galactic and extragalactic HII regions by Henry et al. (2000) is shown in a black dotted line. We omit all uncertainties for visual clarity. The Sun, at (0, 0) on this plot by definition, is marked by a large red star.

abundances are determined, this [N/O]-[O/H][4] relation is more or less the same across a wide range of astrophysical environments. Here we are interested in the origin of both the shape and scatter in this trend.

N is not unique in that perhaps the largest source of uncertainty in understanding its abundances is that accurate and precise nucleosynthetic yields from various enrichment channels remain elusive. Presently, no combination of models for nucleosynthesis in and explosions of massive stars is able to reproduce the observed abundance pattern of the elements, and N is no exception (Griffith et al. 2021). Recently, Grisoni, Matteucci & Romano (2021) argued that rotating massive stars play a key role in establishing the N abundances seen in metal-poor stars in the Milky Way. Rotation has a considerable impact on the N yields of massive stars, because the internal mixing that it causes (Zahn 1992; Maeder & Zahn 1998; Lagarde et al. 2012) brings internally produced C and O nuclei into the H-burning shell where they can be processed into ^{14}N via the CNO cycle (Heger & Woosley 2010; Frischknecht et al. 2016; Andrews et al. 2017). We find similar results here comparing various theoretical models for massive star nucleosynthesis (see discussion in § **??**).

Theoretical models for AGB star nucleosynthesis predict N yields to vary as a function of progenitor mass and metallicity (Cristallo et al. 2011, 2015; Karakas 2010; Karakas & Lugaro 2016; Karakas et al. 2018; Ventura et al. 2013, 2014, 2018, 2020). In sufficiently massive AGB stars, the base of the convective envelope is hot enough to activate proton capture reactions, allowing the CNO cycle to convert C and O isotopes in ^{14}N: a process known as hot bottom burning (HBB). AGB stars are also known to experience thermal pulsations, and with each pulse the convective envelope penetrates into the CO-rich core, bringing some of this material into the envelope: a process known as third dredge-up (TDU)[5]. When both processes are active, each TDU episode adds new seed nuclei for HBB to turn into ^{14}N, substantially increasing the N yields. We demonstrate in §§ **??** and **??** that various theoretical models predict significantly different N yields for high mass AGB stars as a consequence of how TDU and HBB occur in the models. The differences in these processes are in turn a consequence of the microphysical assumptions built into the stellar evolution models (e.g. mass loss, opacity, convection and convective boundaries, nuclear reaction networks).

[4] We follow standard notation where [X/Y] ≡ $\log_{10}(X/Y) - \log_{10}(X/Y)_\odot$.

2 ACKNOWLEDGEMENTS

We are grateful to Amanda Karakas for valuable discussion on the physical processes affecting N production in asymptotic giant branch stars. We thank Paolo Ventura for providing asymptotic giant branch star yields at a wide variety of progenitor metallicities. We acknowledge valuable discussion with Jennifer Johnson, Adam Leroy, Grace Olivier, Amy Sardone, Jiayi Sun, Todd Thompson, and other members of The Ohio State Astronomy Gas, Galaxies, and Feedback group. This work was supported by National Science Foundation grant AST-1909841. D.H.W. is grateful for the hospitality of the Institute for Advanced Study and the support of the W.M. Keck Foundation and the Hendricks Foundation. F.V. acknowledges the support of a Fellowship from the Center for Cosmology and Astroparticle Physics at The Ohio State University.

[5] Here the time adverbial "third" refers only to the fact that these dredge-up episodes are occurring while the star is on the asymptotic giant branch. There is a first TDU, a second TDU, a third TDU, and so on.

REFERENCES

Andrews B. H., Weinberg D. H., Schönrich R., Johnson J. A., 2017, ApJ, 835, 224
Belfiore F., et al., 2017, MNRAS, 469, 151
Berg D. A., et al., 2012, ApJ, 754, 98
Berg D. A., Skillman E. D., Croxall K. V., Pogge R. W., Moustakas J., Johnson-Groh M., 2015, ApJ, 806, 16
Berg D. A., Pogge R. W., Skillman E. D., Croxall K. V., Moustakas J., Rogers N. S. J., Sun J., 2020, ApJ, 893, 96
Bundy K., et al., 2015, ApJ, 798, 7
Cristallo S., et al., 2011, ApJS, 197, 17
Cristallo S., Straniero O., Piersanti L., Gobrecht D., 2015, ApJS, 219, 40
Dopita M. A., Kewley L. J., Sutherland R. S., Nicholls D. C., 2016, Ap&SS, 361, 61
Frischknecht U., et al., 2016, MNRAS, 456, 1803
Gilroy K. K., 1989, ApJ, 347, 835
Griffith E. J., Sukhbold T., Weinberg D. H., Johnson J. A., Johnson J. W., Vincenzo F., 2021, arXiv e-prints, p. arXiv:2103.09837
Grisoni V., Matteucci F., Romano D., 2021, arXiv e-prints, p. arXiv:2109.03642
Gronow S., Cote B., Lach F., Seitenzahl I. R., Collins C. E., Sim S. A., Roepke F. K., 2021a, arXiv e-prints, p. arXiv:2103.14050
Gronow S., Collins C. E., Sim S. A., Röpke F. K., 2021b, A&A, 649, A155
Heger A., Woosley S. E., 2010, ApJ, 724, 341
Henry R. B. C., Edmunds M. G., Köppen J., 2000, ApJ, 541, 660
Hurley J. R., Pols O. R., Tout C. A., 2000, MNRAS, 315, 543
Izotov Y. I., Thuan T. X., Guseva N. G., 2012, A&A, 546, A122
James B. L., Koposov S., Stark D. P., Belokurov V., Pettini M., Olszewski E. W., 2015, MNRAS, 448, 2687
Johnson J. A., 2019, Science, 363, 474
Karakas A. I., 2010, MNRAS, 403, 1413
Karakas A. I., Lugaro M., 2016, ApJ, 825, 26
Karakas A. I., Lugaro M., Carlos M., Cseh B., Kamath D., García-Hernández D. A., 2018, MNRAS, 477, 421
Kodama T., Arimoto N., 1997, A&A, 320, 41
Korn A. J., Grundahl F., Richard O., Mashonkina L., Barklem P. S., Collet R., Gustafsson B., Piskunov N., 2007, ApJ, 671, 402
Lagarde N., Decressin T., Charbonnel C., Eggenberger P., Ekström S., Palacios A., 2012, A&A, 543, A108
Larson R. B., 1974, MNRAS, 166, 585
Lind K., Korn A. J., Barklem P. S., Grundahl F., 2008, A&A, 490, 777
Maeder A., Meynet G., 1989, A&A, 210, 155
Maeder A., Zahn J.-P., 1998, A&A, 334, 1000
Padovani P., Matteucci F., 1993, ApJ, 416, 26
Pilyugin L. S., Vílchez J. M., Thuan T. X., 2010, ApJ, 720, 1738
Rogers N. S. J., Skillman E. D., Pogge R. W., Berg D. A., Moustakas J., Croxall K. V., Sun J., 2021, ApJ, 915, 21
Skillman E. D., Berg D. A., Pogge R. W., Moustakas J., Rogers N. S. J., Croxall K. V., 2020, ApJ, 894, 138
Souto D., et al., 2018, ApJ, 857, 14
Souto D., et al., 2019, ApJ, 874, 97
Suliga A. M., Shalgar S., Fuller G. M., 2020, arXiv e-prints, p. arXiv:2012.11620
Ventura P., Di Criscienzo M., Carini R., D'Antona F., 2013, MNRAS, 431, 3642
Ventura P., di Criscienzo M., D'Antona F., Vesperini E., Tailo M., Dell'Agli F., D'Ercole A., 2014, MNRAS, 437, 3274
Ventura P., Karakas A., Dell'Agli F., García-Hernández D. A., Guzman-Ramirez L., 2018, MNRAS, 475, 2282
Ventura P., Dell'Agli F., Lugaro M., Romano D., Tailo M., Yagüe A., 2020, A&A, 641, A103
Vincenzo F., Matteucci F., de Boer T. J. L., Cignoni M., Tosi M., 2016, MNRAS, 460, 2238
Vincenzo F., et al., 2021, arXiv e-prints, p. arXiv:2106.03912
Zahn J. P., 1992, A&A, 265, 115

Appendices

A `VICE`

`VICE`[1] is an open-source `PYTHON` package designed to model chemical enrichment processes in galaxies with a generic, flexible model. With this paper, we mark the release of version 1.3.0 which presents a handful of new features:

(i) Users may select a mass-lifetime relation for stars from a list of several parameterized forms taken from the literature. Previously, only a single power-law was implemented, but this formulation underestimates lifetimes for stars with masses $\gtrsim 4 M_{\odot}$; now, the options include the equations presented in:

- Vincenzo et al. (2016)
- Hurley, Pols & Tout (2000)
- Kodama & Arimoto (1997)
- Padovani & Matteucci (1993)
- Maeder & Meynet (1989)
- Larson (1974) **(default)**

Generally, chemical evolution models make similar predictions with each of these different forms of the mass-lifetime relation since their quantitative predictions are not considerably different from one another (see the section titled "Single Stellar Populations" under `VICE`'s science documentation for further discussion[2]). We select the Larson (1974) form as a default within `VICE` because it is typical compared to the others and requires the lowest amount of computational overhead (aside from the single power-law option).

(ii) We have added two additional tables of AGB star yields sampled at various progenitor masses and metallicities: the KL16+K18 and V13 models presented in this paper are new to `VICE` (see discussion in § **??** for details).

(iii) We have built in the SN Ia yields presented in Gronow et al. (2021b,a). These tables present yields for double detonations of sub-Chandrasekhar mass carbon-oxygen white dwarfs at various progenitor metallicities.

Although `VICE` includes built in SN and AGB star yield tables, users are not required to adopt any one of them for use in their chemical evolution models. Instead, it allows arbitrary functions of metallicity for both CCSN and SN Ia yields and functions of progenitor mass and metallicity for AGB star yields. It provides similar flexibility for additional parameters typically built into GCE models. `VICE`'s backend is implemented entirely in ANSI/ISO `C`, providing it with the powerful computing speeds of a compiled library while retaining such scientific flexibility within the easy-to-use framework of `PYTHON`.

Requiring a Unix kernel, `VICE` supports Mac and Linux operating systems; Windows users should install and use `VICE` entirely within the Windows Subsystem for Linux. On machines with x86_64 hardware, it can be installed in a terminal via `pip install vice`. Users running ARM64 hardware (e.g. Macintosh computers with Apple's new M1 processor) must install `VICE` by compiling from source, instructions for which can be found in the documentation. After installing, running `vice --docs` and `vice --tutorial` from a `Unix` terminal will launch a web browser to the documentation and to a

[1] Install (PyPI): `https://pypi.org/project/vice`
Documentation: `https://vice-astro.readthedocs.io`
Source Code: `https://github.com/giganano/VICE.git`
[2] `https://vice-astro.readthedocs.io/en/latest/science_documentation/`

jupyter notebook intended to familiarize first time users with `VICE`'s API.